

See discussions, stats, and author profiles for this publication at: <https://www.researchgate.net/publication/40036421>

Biocatalysis with Thermostable Enzymes: Structure and Properties of a Thermophilic 'ene'-Reductase related to Old Yellow Enzyme

ARTICLE *in* CHEMBIOCHEM · JANUARY 2010

Impact Factor: 3.09 · DOI: 10.1002/cbic.200900570 · Source: PubMed

CITATIONS

55

READS

50

7 AUTHORS, INCLUDING:



Björn Vidar Adalbjörnsson

Matis ltd. / University of Iceland

4 PUBLICATIONS 69 CITATIONS

SEE PROFILE



Christopher Pudney

The University of Manchester

22 PUBLICATIONS 438 CITATIONS

SEE PROFILE



Thomas A Jowitt

The University of Manchester

57 PUBLICATIONS 934 CITATIONS

SEE PROFILE



Nigel S Scrutton

The University of Manchester

346 PUBLICATIONS 7,760 CITATIONS

SEE PROFILE

Biocatalysis with Thermostable Enzymes: Structure and Properties of a Thermophilic 'ene'-Reductase related to Old Yellow Enzyme

Björn V. Adalbjörnsson,^[a] Helen S. Toogood,^[a] Anna Fryszkowska,^[b] Christopher R. Pudney,^[a] Thomas A. Jowitt,^[c] David Leys,^[a] and Nigel S. Scrutton^{*,[a]}

We report the crystal structure of a thermophilic "ene" reductase (TOYE) isolated from *Thermoanaerobacter pseudethanolicus* E39. The crystal structure reveals a tetrameric enzyme and an active site that is relatively large compared to most other structurally determined and related Old Yellow Enzymes. The enzyme adopts higher order oligomeric states (octamers and dodecamers) in solution, as revealed by sedimentation velocity and multiangle laser light scattering. Bead modelling indicates that the solution structure is consistent with the basic tetrameric structure observed in crystallographic studies and electron microscopy. TOYE is stable at high temperatures ($T_m >$

70 °C) and shows increased resistance to denaturation in water-miscible organic solvents compared to the mesophilic Old Yellow Enzyme family member, pentaerythritol tetranitrate reductase. TOYE has typical ene-reductase properties of the Old Yellow Enzyme family. There is currently major interest in using Old Yellow Enzyme family members in the preparative biocatalysis of a number of activated alkenes. The increased stability of TOYE in organic solvents is advantageous for biotransformations in which water-miscible organic solvents and biphasic reaction conditions are required to both deliver novel substrates and minimize product racemisation.

Introduction

The use of enzymes as biocatalysts in asymmetric synthesis has become an established manufacturing route^[1] due to their often high efficiency, as well as the stereo- and enantioselectivity of their reactions.^[2] While enzymes can be found to catalyse reactions of industrial importance, they rarely have properties required for large-scale chemical production such as high activity and selectivity for non-natural substrates.^[3] In addition, chemical synthesis is often carried out in the presence of organic solvents and high substrate conditions, and these are often inhibitory to enzymes.^[2]

Reactions carried out at high temperatures can be advantageous in cases in which the substrate or product has poor solubility at low temperatures and/or the thermodynamics of the reaction causes higher yield at higher temperatures. In addition, biotransformations in the presence of organic solvents might lead to a change in enantioselectivity of the reaction, reversal of the thermodynamic equilibrium of hydrolysis reactions and suppression of water-dependent side reactions.^[4] Thermo- and hyperthermophilic enzymes have great potential for industrial use as their high resistance is not only to temperature, but can also be towards chemicals, organic solvents and extreme pH values at ambient temperatures.^[5–7]

The biocatalytic potential of the Old Yellow Enzyme family (OYE; EC 1.6.99.1) in the reduction of industrially useful activated α,β -unsaturated alkenes has been studied extensively.^[8–11] These NAD(P)H-dependent oxidoreductases are useful catalysts in the reduction of α,β -unsaturated ketones, aldehydes, nitroalkenes, carboxylic acids and derivatives, yielding products with a variety of biotechnological and pharmaceutical applica-

tions.^[8–10, 12–18] Members of this family include OYE1 (brewers yeast),^[19] pentaerythritol tetranitrate reductase (PETNR; *Enterobacter cloacae* PB2),^[20] morphinone reductase (MR; *Pseudomonas putida* M10),^[21] 12-oxophytodienoate reductase 1 (OPR1; tomato)^[22] and YqjM (*Bacillus subtilis*).^[23] These enzymes have structures based on an eight-stranded α/β barrel fold (TIM barrel),^[24] and can exist as a functional monomer (for example, PETNR),^[20] dimer (for example, MR)^[25] or tetramer (YqjM).^[26]

A search of the available sequence databases for potential OYE family members from thermophilic microorganisms led us to TOYE, a hitherto uncharacterised NAD(P)H-dependent oxidoreductase from *Thermoanaerobacter pseudethanolicus* E39.^[27] Here we describe the characterisation and biocatalytic potential of its "ene-reductase" activity, as well as the crystal structures of the apo and nicotinamide cofactor analogue-bound TOYE. We provide evidence that TOYE is the first known OYE

[a] B. V. Adalbjörnsson, Dr. H. S. Toogood, Dr. C. R. Pudney, Dr. D. Leys, Prof. N. S. Scrutton
Faculty of Life Sciences, University of Manchester
131 Princess Street, Manchester M1 7DN (UK)
Fax: (+44) 161-306-8918
E-mail: nigel.scrutton@manchester.ac.uk

[b] Dr. A. Fryszkowska
School of Chemistry, University of Manchester
131 Princess Street, Manchester M1 7DN (UK)

[c] Dr. T. A. Jowitt
Faculty of Life Sciences, University of Manchester
Michael Smith Building, Oxford Road, Manchester M13 9PT (UK)

Supporting information for this article is available on the WWW under <http://dx.doi.org/10.1002/cbic.200900570>.

to exist in solution in large complexes of multiple oligomeric states (for example, tetramers, octamers). The unique structural features of TOYE are discussed with reference to both its thermostability and biocatalytic potential.

Results and Discussion

General

We performed a database search for OYE enzymes from thermophilic microorganisms in an effort to find a more stable OYE for industrial biotransformations. TOYE (thermostable OYE) from *T. pseudethanolicus* E39^[27] was chosen, and recombinant forms of the protein (native and His₆-tagged) were produced at high yield and purity (Figure S1 in the Supporting Information).

An alignment of eight OYE sequences (Figure S2) belonging to the two family subclasses^[26] shows each contain unique sequence and structural features. TOYE belongs to the YqjM subclass, and sequence comparisons suggest two other enzymes from thermophilic microorganisms belong to this subclass, namely the putative NADH-dependent oxidoreductase enzymes from *Geobacillus kaustophilus* HTA426,^[28] and *Coprothermobacter proteolyticus*.^[29] Given that YqjM was originally isolated from the mesophilic *B. subtilis*,^[23] we describe this subclass as “thermostable-like” OYEs in comparison to “classical” OYEs such as PETNR and OYE1.

Overall structure of TOYE

We determined the X-ray crystal structures of both holo-TOYE (His₆-tagged) and OYE inhibitor 1,4,5,6-tetrahydroNAD (NADH₄)-bound enzyme to high resolution (1.6 and 1.8 Å, respectively). The data collection and refinement statistics can be found in Table 1. Both structures show a homotetrameric arrangement composed of a dimer of dimers (Figure 1A; Figure S3A–B). Each monomer is comprised of a compact domain of an (α/β)₈-barrel fold (TIM barrel), typical for OYE enzymes.^[24–26,30] Both structures are virtually identical, and are very similar to the other known tetrameric OYE YqjM (50% sequence identity),^[26] with RMSD values of 0.259 and 0.924, respectively. However, the angle of interaction between monomers within the functional dimers of TOYE and YqjM differ with a typical separation distance of about 2 Å (Figure 1A). Other significant backbone changes between TOYE and YqjM are highlighted in Figure 1A.

Subunit interactions

Like YqjM, the tetramer contains a water-filled central hole or cavity, with the active sites opening into this cavity. The (α/β)₈-domains (YqjM numbering of helices and sheets throughout)^[26] of each monomer within the functional dimer interact with each other with same sides facing. As a consequence, a network of hydrogen bonds that involve the same residues from both subunits, holds the monomers together. Residues involved in this interaction include the C-terminal residues Q330,

Table 1. X-ray crystallographic data collection and refinement statistics.

Parameters	TOYE-His ₆ ^[a]	TOYE-NADH ₄ ^[a]
Space group	P2 ₁	P2 ₁
Cell dimensions		
a, b, c (Å)	86.93, 97.38, 94.39	87.38, 98.56, 95.13
α, β, γ (°)	90.00, 92.34, 90.00	90.00, 92.40, 90.00
Resolution (Å)	64.8–1.6	68.4–1.8
	(1.64–1.60)	(1.85–1.80)
R _{merge} (%)	6.4 (35.1)	10.9 (30.2)
I/σI	11.7 (3.0)	11.0 (4.4)
Completeness (%)	98.9 (95.0)	98.9 (99.4)
Redundancy	2.8 (3.0)	3.3 (3.4)
Unique reflections	189 805	141 968
R _{work} /R _{free}	15.2/17.9	15.5/19.4
	(22.5/25.6)	(18.5/21.8)
RMS deviations		
Bond angles (°)	1.295	1.289
Bond lengths (Å)	0.010	0.012
Ramachandran plot		
Allowed region (%)	96.2	96.3
Additionally allowed region (%)	3.7	3.7

[a] Highest resolution shell is shown in parentheses. $R_{\text{merge}} = \frac{\sum_i \sum_j |I_i(hkl) - \langle I(hkl) \rangle|}{\sum_i \sum_j I_i(hkl)}$, where $I_i(hkl)$ is the intensity of the i th observation of unique reflection hkl . Redundancy = total number of reflections/total unique reflections. $R_{\text{work}} = \frac{\sum ||F_{\text{obs}}| - |F_{\text{calc}}||}{\sum |F_{\text{obs}}|}$, where F_{obs} and F_{calc} are observed and model structure factors, respectively. R_{free} was calculated by using a randomly selected set (5%) of reflections.

Y331 and A334 (backbone O), which are highly conserved within the thermostable-like subclass, but not classical OYEs. In addition, T45 residues of both subunits (S46 in YqjM) interact through their OG1 atoms as well as side chain interactions between S28/H42/R46 and Q330/Y331/Y315. The total interaction surface is 1054 Å² with a complexation significance score (CSS)^[32] of 1.0; this is consistent with a functional interaction. While the nature of these interactions is similar in YqjM, the C-terminal portion of TOYE encompassing helices 8–F is significantly different in backbone orientation (Figure 1A). This region forms an “arm” that interacts with the active site of its neighbouring monomer to form the functional dimer. In YqjM, the loop is extended by three amino acids, and is oriented towards the turn T287M291 of the adjacent subunit. Residues Q323 and L324 (absent in TOYE) interact with residues G289 and R3, respectively, of the adjacent subunit. In TOYE, the equivalent loop is reoriented towards the central cavity so these interactions are not possible and the C-terminus is disordered within the central cavity. In spite of the loop differences, TOYE still contains the key “arginine finger”^[26] R333 (R336 in YqjM), involved in substrate binding which extends into the active site of the adjacent monomer close to the flavin. In the holo-enzyme, the density of this residue suggests there are at least three orientations of the side chain (results not shown). The density of at least one position of R333 clashes significantly with the FMN; this likely reflects the observation that the recombinant enzyme is not fully flavinated (FMN occupancy approximately 69%). In NADH₄-TOYE the density for most of the side chain in all but subunit B is disordered. This inherent

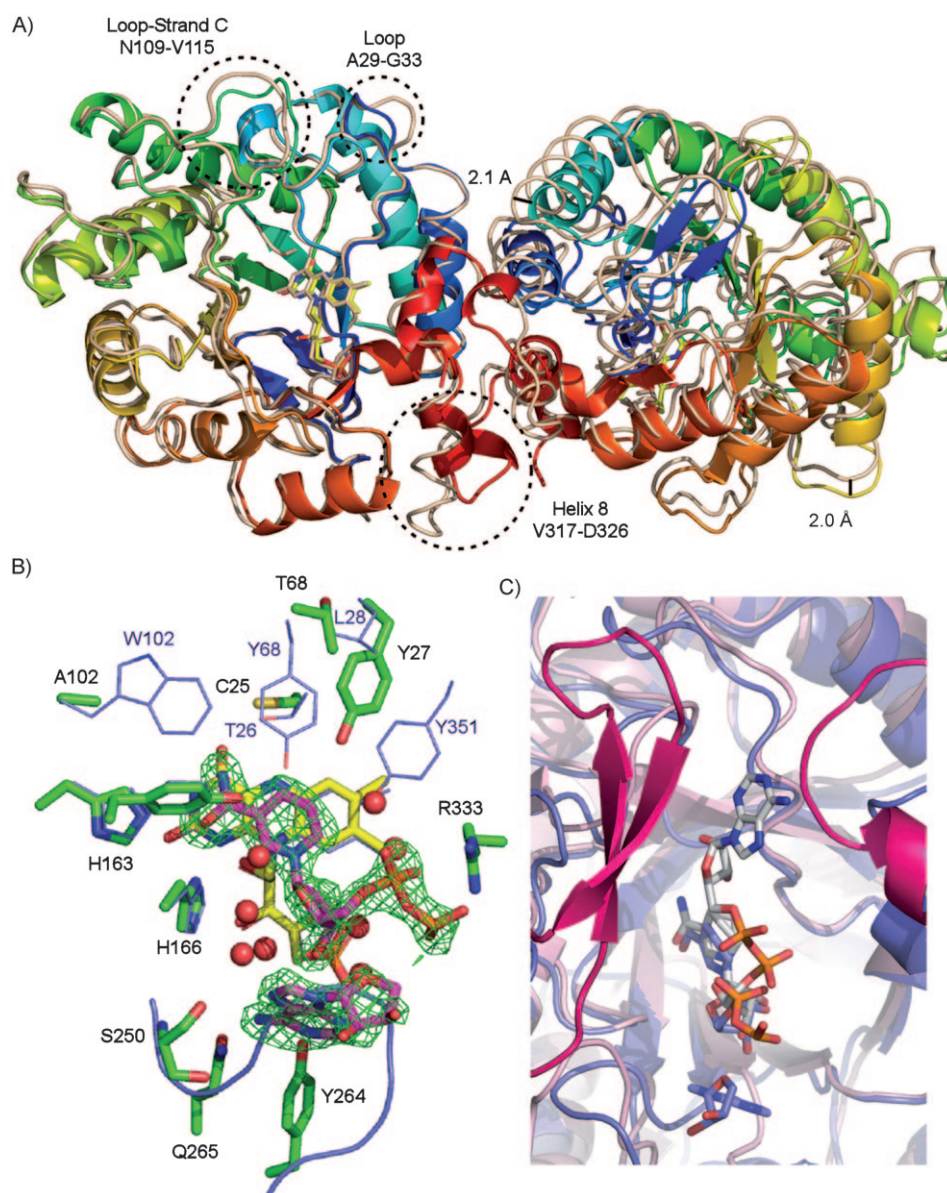


Figure 1. X-ray crystal structures of TOYE. A) Superimposition of functional dimers of TOYE-His₆ and YqjM (PDB code 1Z41). TOYE is shown as a rainbow-coloured cartoon from N- (blue) to C-terminus (red) while YqjM is shown as a pale pink ribbon. Helix and residue numbering refers to the YqjM and TOYE structures, respectively. B) Position of the bound NADH₄ cofactor in the active site of TOYE superimposed with the PETNR structure (PDB code 1H50). The omit $|F_o| - |F_c|$ map of NADH₄ is contoured at three σ (green mesh). TOYE residues and NADH₄/FMN are shown as coloured sticks with green and magenta/yellow carbons, respectively, while water is shown as red spheres. PETNR residues are shown as coloured lines with blue carbons. Residues of PETNR that differ in amino acid identity are labelled. PETNR residues forming a loop overlapping the adenosyl-portion of the NADH₄ binding site are shown as a blue ribbon. C) Superimposition of TOYE and MR at the NADH₄ binding regions between two monomers. The two NADH₄ molecules are shown as coloured sticks with magenta and grey carbons for TOYE and MR, respectively. TOYE and MR are shown as blue and pale pink cartoons, respectively. The two bright pink loops refer to MR residues absent in TOYE that are involved in creating a surface groove where NADH₄ is positioned. All figures were generated in Pymol.^[31]

flexibility might have a functional consequence to enable it to interact with a wide range of substrates.

The interactions between nonfunctional dimers involve helix 7 (residues 287–300) of both subunits as well as helix 6 residues (Y261K274) of one subunit and Y261V266 of the adjacent subunit. These interactions encompass both hydrophobic interactions (for example, Y261, P262, Y264 and L291) as well

as extensive hydrogen bonds between the same residues on opposite monomers (Y261, G263, K267, T287, T288, E290 and N298). In addition, salt bridges are present and involve residues K267, E270 and R300. The electron density for both E270 and R300 shows two distinct conformations of each, with R300 of each subunit interacting with one conformation of the other; this results in a “diamond” pattern of the two interactions (results not shown). The total interaction surface is only 776 Å² and has a CSS value of only 0.325.^[32]

Active site

Both TOYE and YqjM contain large, easily accessible hydrophobic active sites, with substrate entry through the central cavity.^[26] This differs from the classical OYEs that have significantly smaller active sites due to the shortening and reorientation of β -strand 6 to the turn before β -strand 7, as well as a reorientation of the slightly larger turn between β -strand 5 and α -helix 5 (Figure 1B). The active site contains a noncovalently bound FMN molecule (Figures 1B, S3C), in a position similar to other OYEs, with its *si*-face directed towards the solvent. The isoalloxazine ring exhibits a nonlinear “butterfly-bend” shape as seen in YqjM.^[26] The interactions between the FMN and the surrounding protein/solvent are extensive (Table S1), and are similar to those in YqjM. Differences include backbone interactions between P23 and C25 with FMN N1 and N5 atoms, respectively,

while in YqjM N1 and N3 interact with the highly conserved substrate-binding residues H167 and H164 (H166 and H163 in TOYE), respectively. The electron density for the FMN showed it was partially occupied (80%) with minor additional density for an alternative conformation of the ribityl chain, except for the terminal phosphate atoms that are anchored in place by multiple interactions (Table S2).

The omit map $|F_o| - |F_c|$ electron density suggests a small molecule such as a formate or acetate ion might be bound on the *si*-face of the isoalloxazine ring of FMN compared to the presence of a sulphate ion in YqjM.^[26] Therefore an acetate molecule has been modelled into each subunit of holo-TOYE (Figure S3C), in a position similar to holo-PETNR (PDB code: 1H50),^[33] although the density suggests some mobility of the molecule. In this position, an acetate oxygen atom interacts with both H163 NE2 and H166 ND1 and the other oxygen with water molecule/s (Figure S3C/Table S1).

A superimposition of members of the two subclasses of OYE (TOYE and PETNR) show some important differences in the residue composition lining the active site (Figure 1B) that are often highly conserved within each subclass. The key substrate binding residues H163/H166 were conserved within the TOYE subclass, but were sometimes a histidine/asparagine pair (H186/N189; MR numbering) in classical OYEs. The putative proton donor is highly conserved (Y168; TOYE numbering) while the conserved Y351 involved in substrate/inhibitor binding of classical OYEs is absent in the smaller molecular mass TOYE subclass. Interestingly, residue Y27 is located near Y351 (PETNR), and is only conserved in thermostable-like OYEs. The highly conserved T26 (PETNR numbering), known to interact with the FMN N3 atom, has been replaced by a cysteine in the TOYE subclass. Two other highly conserved hydrophobic residues W102 and Y68 (PETNR numbering), have been replaced by smaller amino acids alanine/glycine and threonine/serine, respectively, with lower sequence conservation. The differences and conservation in the nature of the residues in the active site between the two subclasses likely reflects the substrate binding and/or shape and size of the active site. In particular, the substitution of W102 in PETNR for alanine in TOYE might be important in substrate binding as seen in recent work in OYE1 yielded enzymes with altered stereochemical outcomes.^[15]

Inhibitor binding

The omit map $|F_o| - |F_c|$ electron density of the NADH₄-bound TOYE crystal structure showed clear density for the inhibitor, except for the phosphate atom O5' and the adjacent carbon atom C5' in subunit B, which is disordered in this structure (Figure 1B). In the remaining subunits there is poor density for the adenosyl ribose so it was only modelled into subunit B. The inhibitor makes multiple interactions between both the protein and the solvent (Table S2). The highly conserved H163 and H166 residues interact with the carbonyl oxygen of the nicotinamide moiety, while residues Y264, Q265 and S250 interact with the N6A and N7A atoms of the adenine base. In this position, the nicotinamide atom C4N (equivalent to the hydride transferring carbon in NAD(P)H) is within 3.7 Å of the FMN N5 atom. Additional interactions include a hydrogen bond between the O2' atom of the adenosyl ribose and the backbone O of V256. A significant difference between the holo- and NADH₄-bound structures is the position of the "arginine finger" R333 the side chain atoms NH1/NH2 of which in-

teract with both phosphate groups through O1P/O1N atoms of NADH₄ in chains B and D (side chain is more disordered in chains A and C). However, the quality of the density of the later ribose suggests a higher mobility than the adjacent phosphate atoms; this is likely due to its location on the surface of the central cavity.

A combination of these interactions cause the inhibitor to fold back upon itself at the solvent-exposed central cavity interface; this would position both the adenosine base and its ribose directly beneath the D-ribose ring, with no density seen for the adjoining atoms C5' and O5'. We modelled one of the possible positions of the O5' and C5' in subunit B and found some constraint in the C4'–C5'–O5' bond angle, although it was within the allowable range (results not shown). These constraints are likely a consequence of the multiple interactions holding both ends of the inhibitor in position. The poorer density for the adenosyl ribose in the remaining subunits and the absence of density for C5' in all subunits reflects the higher mobility of the adenosyl portion of the inhibitor in this solvent-exposed region.

These interactions are in stark contrast to the orientation of binding of NADH₄ to the classical OYE MR,^[34] in which the phosphate atoms have reoriented; this causes both the ribose and its adenine base to lie above the nicotinamide portion within a solvent-exposed groove on the surface of the protein (Figure 1C). While the interactions with NADH₄ in this region are purely through the solvent, this groove is surrounded by two "loops," the size and orientation of which differ significantly in the thermostable OYE subclass. Importantly, the small β-strand C between β-strand 3 and α-helix 3 is considerably elongated in classical OYEs, and this allows the "loop" to form. Secondly, the differences in the highly conserved C-terminal loop Q330–A334, which is not conserved in classical OYEs, causes a change in the orientation of this loop compared to MR. However, the position of the nicotinamide moiety in MR is similar to TOYE, with interactions between the equivalent H186/N189 residues (MR) with the carbonyl-oxygen, and a third interaction between the substrate interacting residue Y356 (absent in TOYE) and the pyrophosphate moiety. Interestingly, the inhibitor is unlikely to bind to classical OYEs, such as PETNR, in a TOYE-like manner due to the altered position and elongation of β-strand 6 that would overlap with the adenosine portion of NADH₄ in TOYE (blue ribbon in Figure 1B).

Oligomeric states of TOYE

Both SDS PAGE and native PAGE analysis of TOYE showed the presence of multiple bands, which were positively identified to be TOYE. This suggests TOYE exists *in vitro* in multiple oligomeric states. To investigate this phenomenon we performed multi-angle laser light scattering (MALLS) and sedimentation velocity analysis on TOYE (Figure 2A; Table S3). These results clearly showed the minimal quaternary structure of TOYE to be a tetramer, but also higher species such as octamers and dodecamers were present in lower proportions according to MALLS and native PAGE, respectively (Figure 2A–B). Both methods also detected a very minor species of a hexamer,

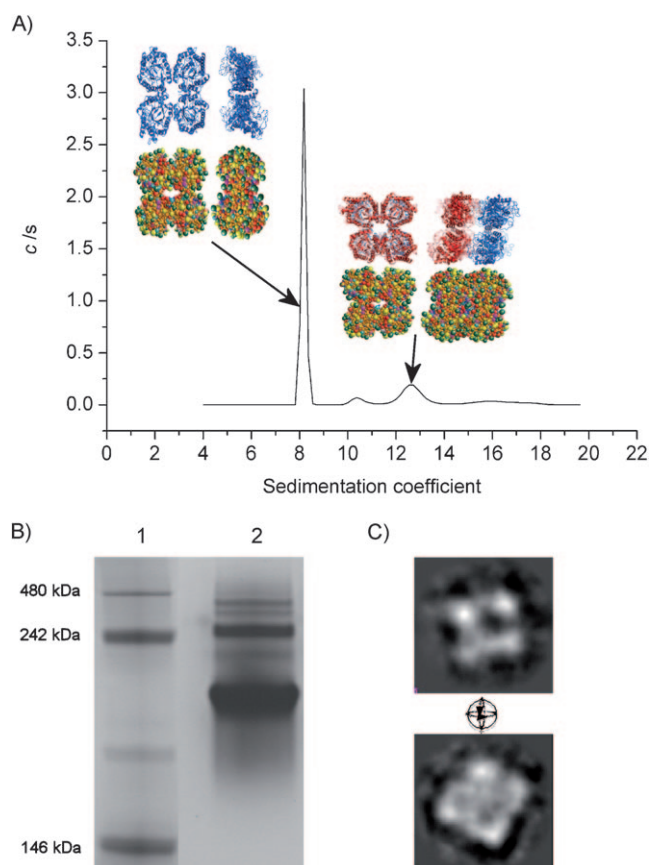


Figure 2. A) MALLS analysis of TOYE-His₆. Inset: Bead models of the quaternary structures for TOYE were generated by using the PDB file and the SOMO solution bead modelling program.^[35] The crystal structure oligomers are shown as cartoons and were arranged in several orientations by using Pymol.^[31] B) Native PAGE analysis of TOYE-His₆. Lane 1 = native PAGE molecular mass markers (Invitrogen) with the masses of the proteins indicated to the left of the lane. Lane 2 = TOYE. C) Two selected reference free projection averages of tetrameric/octameric TOYE calculated from a complete dataset (N = 1450) with likely top-view (above) and side-view (below) projections. Scale: the width of each box is 25 nm.

which is presumed to be due to partially unfolded protein and/or incorrectly assembled multimers. This is the first example of an OYE demonstrated to exist *in vitro* in a higher order than a tetramer.

We performed bead modelling of the tetramer and octamer to ascertain if the hydrodynamics data were consistent with the crystal structure (Figure 2A inset). The modelled tetramer had an area of 108 nm², consistent with the crystal structure. Modelled radii (R_H) and sedimentation coefficients (S^0) of both the tetramer and octamer are consistent with experimental data (Table S3). Some models of the octamer were rejected based on poor fitting to the hydrodynamic data (Figure S4). The modelled octamer is assembled as a dimer of tetramers with the central hole remaining intact. We also analysed TOYE by transmission electron microscopy (TEM), which showed a homogeneous population of clear squared single particles with a diameter of 10–11 nm (Figures 2C, S5). Image analysis of the data identified a particle with clear C₄ rotational symmetry with a corresponding projection with a similar diameter, but a

clear axis of pseudo mirror symmetry. There was no evidence for elongation of the basic tetramer into fibres or extended chains. These data are consistent with a basic tetrameric particle that forms a 2-layered stack with a probable D-symmetrical arrangement of rotational and flipped axes, consistent with the bead modelling.

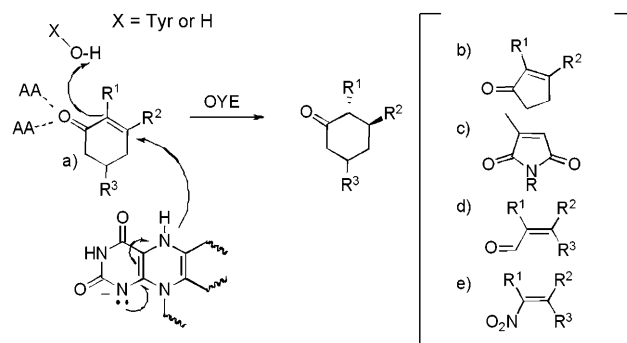
Solvent stability of TOYE

We investigated the thermostability of TOYE by monitoring the secondary structure unfolding/aggregation with circular dichroism (CD), differential scanning calorimetry (DSC) and fluorescence changes of FMN/Trp residues in TOYE (Figures S6–S7 and see discussion of “Thermostability determinants of TOYE” in the Supporting Information). Observations with other enzyme systems suggest that thermo- and hyperthermophilic enzymes tend to have higher stability towards organic solvents at ambient temperatures.^[36–39] We therefore compared the stability of both the mesophilic PETNR and thermophilic TOYE in the presence of water-miscible organic solvent:aqueous buffer systems by using steady-state kinetics methods (Figure S8).

Steady-state reactions in the presence of ethanol showed a steady decline in reaction rate with increasing solvent concentration for both TOYE and PETNR (Figure S8), with 50% loss at approximately 45% and 20% ethanol, respectively. PETNR precipitated significantly above 40% ethanol, while remarkably TOYE still maintained approximately 20% of its activity in 80% ethanol. In addition, the complete recovery of activity of TOYE after a preincubation in up to 70% ethanol shows a dramatic increase in solvent stability of TOYE compared to PETNR. This can potentially be exploited in industrial biotransformations in which organic solvents are often used to increase substrate solubility and decrease unfavourable water-dependent reactions.

Substrate specificity

Members of the OYE family typically catalyse C=C bond reduction of α,β -unsaturated ketones, aldehydes, nitroalkenes, carboxylic acids and derivatives^[8–10,12–18] through a net *trans*-addition of 2H^[40] (Scheme 1). To benchmark the biocatalytic



Scheme 1. General mechanism and stereochemistry of α,β -unsaturated substrate reduction by OYEs. a) Substrates 4a–9a; b) Substrates 1a–3a; panel c) Substrates 10a–11a; d) Substrates 12a–15a; e) Substrate 18a.

potential of TOYE against other OYEs, we investigated the anaerobic reduction of a variety of α,β -unsaturated activated olefins. Initially, we determined the kinetic constants of the reductive half-reactions (k_{lim} and k_s) with NAD(P)H (Table S4 and Figure S5) and steady-state parameters (apparent k_{cat}/K_M) with oxidising substrates to determine the substrate specificity of TOYE (Table 2).

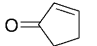
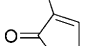
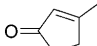
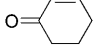
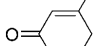
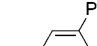
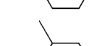
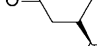
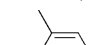
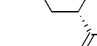
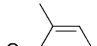
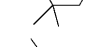
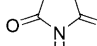
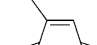
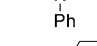
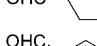
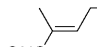
In stopped-flow studies, NADPH preferentially reduces TOYE over NADH, with k_{lim} values of 31.7 ± 2.1 and $2.8 \pm 0.1 \text{ s}^{-1}$, respectively, at 25°C . These results compare to YqjM, which has a comparable k_{lim} value,^[23] although a tenfold higher K_s value than TOYE (Table S4 and Figure S9). In addition, the k_{lim} and K_s values of TOYE-His₆ with NADH at 50°C were $18.4 \pm 0.2 \text{ s}^{-1}$ and $186.1 \pm 8.1 \text{ mM}$, respectively; these values show a greater than sixfold rate acceleration and threefold increased K_s value compared to reactions at 25°C . As the NADH₄-TOYE crystal structure shows a relatively high mobility for the adenosyl-ribose moiety of the NADH analogue, the mechanism of discrimination between NADH and NADPH is not clear.

When His₆-tagged at the C-terminus, TOYE maintains both its tetrameric/octameric structural integrity and its catalytic ability as seen by the near identical kinetic parameters of the reductive half-reaction with NADPH compared to enzyme lacking the His₆ tag (Table S4). This is in contrast to YqjM-His₆, which loses both structural integrity and catalytic efficiency.^[41] These differences might be due to the significant reorientation of the C-terminal region of TOYE (helices 8-F; Figure 1A), which in YqjM are involved in subunit-subunit interactions. The location of the last visible amino acid K336 at the surface of the central cavity in the crystal structure of TOYE suggests the His₆ tag is disordered within this cavity and therefore does not disrupt the quaternary structure.

The steady-state parameters for TOYE with oxidising substrates showed on average lower rates and specificity (k_{cat}/K_M) than PETNR^[42] or YqjM^[26] at 25°C as expected for thermophilic enzyme catalysis at mesophilic temperatures (Table 2). For example, the rate with 2-cyclohexenone **4a** with TOYE at 25°C was $1.18 \pm 0.09 \text{ s}^{-1}$ compared to 6.1 and 4.4 s^{-1} for PETNR and YqjM, respectively.^[26,42] However, at 50°C this rate had increased to $2.29 \pm 0.35 \text{ s}^{-1}$. TOYE showed a marked preference for 2-methyl cyclopentenone **2a** over the 3-methyl substituted substrates **3a**, **5a**, and **6a**, with almost no detectable activity against the latter three substrates (Table 2). This is similar to other OYEs such as OPR1, OPR3 from *Lycopodium obscurum*,^[8] and YqjM, which did not significantly reduce substrates **3a** and **5a**.^[8] In contrast, classical OYEs such as OYE1-3^[14] and PETNR^[42] can reduce substrates **3a** and **5a**, although to a lower yield than the equivalent 2-methyl substituted compounds. A superimposition of the structures of TOYE and PETNR suggests that this lack of activity against 3-methyl substituted substrates by TOYE might be due to a possible clash between the side chain of I67 and the substituent of the substrate, an interaction not possible in PETNR due to a shift in the position of the backbone of the protein chain and the substitution of this residue for glycine.

Like other OYEs,^[8,11,14] TOYE is highly active towards the malimides **10a–11a**, with a slightly lower rate but higher specific-

Table 2. Steady-state kinetics of TOYE with α,β -unsaturated alkene substrates.

Substrate ^[a]	Rate [s^{-1}]	k_{cat}/K_M ^[b] [$\text{s}^{-1} \text{ mM}^{-1}$]
1a 	0.74 ± 0.07	0.6
2a 	0.17 ± 0.01	0.1
3a 	< 0.01	ND
4a 	1.18 ± 0.09 (2.29 ± 0.35)	0.5 (1.9)
5a 	ND	ND
6a 	ND	ND
(5R)- 7a 99% ee 	2.23 ± 0.10	1.5
(5S)- 8a 99% ee 	0.83 ± 0.07	0.6
9a 	0.02 ± 0.01	ND
10a 	26.85 ± 3.02	194.4
11a 	16.90 ± 0.61	213.6
12a 	0.33 ± 0.02	0.3
13a 	0.39 ± 0.01	ND
14a 	0.22 ± 0.01	0.14
15a 	0.04 ± 0.01	0.05
16a 	ND	ND
17a 	< 0.01	ND

[a] Reactions (0.3 mL) were performed in 50 mM $\text{KH}_2\text{PO}_4/\text{K}_2\text{HPO}_4$ pH 7.0 containing 100 μM NADPH, 1 mM oxidising substrate and 0.1–2 μM TOYE for 1 min at 25°C . [b] Specificity constants (apparent k_{cat}/K_M) were determined from the slope of the rate versus substrate concentration plot at substrate concentrations well below the estimated K_M (5–20 μM). ND = No significant activity detected under steady-state conditions.

ity for the phenyl substituted substrate **11a**. These rates were surprisingly higher than PETNR, in spite of the reactions being conducted 44°C below the optimum growth temperature for the source organism (69°C). Other differences include the

relatively poor rate of TOYE towards ketoisophorone **9a** under steady-state conditions; this contrasts with other OYEs, such as PETNR, that have high activity towards this substrate.^[42] TOYE also has a relatively high rate of catalysis with both (5*R*)- and (5*S*)-carvone compared to PETNR. The origin of these differences is likely multifactorial such as the change in the shape and composition of residues lining the active site combined with the differences in the relative flexibility of the thermophilic versus mesophilic proteins.

Stereochemistry of C=C reduction

We carried out biotransformations of TOYE at 30 °C against a variety of activated α,β -unsaturated alkenes, by using NADH as the source of reducing equivalents, to determine the efficiency and enantioselectivity of C=C reduction (Table 3). Like YqjM, the (*S*)-enantiomer of **2b** was produced with moderately high enantioselectivity (70%).

This is the opposite enantiomeric product as expected from Scheme 1, but was also seen with classical OYEs such as PETNR and likely arises from an alternative or “flipped” binding mode of **2a** in the enzyme active site.^[43] Classical OYEs such as OYE1–3 produce racemic mixtures of product **2b** by using NAD(P)H,^[14] while OPR1 and OPR3 produce (*S*)-**2b** with compa-

rable enantiopurities (45–64% *ee*).^[8] The reduced enantiopurity of the products is not surprising given the observation that 2-methyl-substituted products are subject to nonenzymatic racemisation.^[42] However, in the case of YqjM, the use of the cofactor regeneration system NADP⁺/glucose-6-phosphate dehydrogenase (G6PDH) dramatically improved the enantiopurity of the product from 55% (NADH) to 94%,^[8] this highlights the importance of optimising the reaction conditions, including the source of reducing equivalents.

TOYE did not significantly reduce substrates **3a** and **5a**, similar to the enzymes YqjM, OPR1 and OPR3, while other classical OYEs produced low–medium yields of the respective (*S*)-enantiomeric products with > 99% *ee*.^[8,14] The reduction of carvones **7a** to **8a** proceeded with high conversion rates and high enantiopurity (85 to 95% *de* for **8b** and **7b**, respectively), although the product yields were lower than expected. These two diastereoisomeric products had the same configuration on carbon C2 (2*R*; new chiral carbon generated); this suggests that the presence of bulky substituents in this position does not affect the binding mode of the substrate in the active site of TOYE.

The reduction of ketoisophorone **9a** by TOYE yielded the expected (*R*)-**9b** product with a low enantiopurity (26%) as seen with other OYEs.^[8,14] The poor *ee* likely arises from significant

solvent-catalysed racemisation of the product, although recent reaction optimisation studies with PETNR have shown that a reduction of the reaction time (thereby reducing substrate:water exposure time) can dramatically improve the enantiopurity to > 93%.^[42] In the case of YqjM, substitution of NADPH for the cofactor recycling system NADP⁺/G6PDH was sufficient to improve the enantiopurity of (*R*)-**9b** from 37% to 97%.^[8] In comparison, the reduction of the *N*-phenyl substituted maleimide **10a** by TOYE yielded the (*R*)-enantiomer with characteristically high yields and enantiopurity. This is due to both the lack of significant product racemisation and the observation that at least two likely modes of binding of this substrate would yield the same enantiomeric product.^[42]

The reduction of 2-methyl pentenal **14a** proceeded with high efficiency and yield, although with only moderate enantiopurity of (*S*)-**14b** (55%) as seen with PETNR.^[42] Such poor stereoselectivity is

Table 3. Product determination of the reduction of α,β -unsaturated alkene substrates by TOYE.

Substrate	Product ^[a]		Conv. ^[b,c] [%]	Yield ^[c] [%]	<i>ee</i> ^[d] [%]
2a	(<i>S</i>)- 2b		77	73	70
(5 <i>R</i>)- 7a 99% <i>ee</i>	(2 <i>R</i> ,5 <i>R</i>)- 7b 99% <i>ee</i>		94	61	95 <i>de</i>
(5 <i>S</i>)- 8a 99% <i>ee</i>	(2 <i>R</i> ,5 <i>S</i>)- 8b 99% <i>ee</i>		89	77	85 <i>de</i>
9a	(<i>R</i>)- 9b		99	74	26
10a	(<i>R</i>)- 10b		> 99	90	> 99
14a	(<i>S</i>)- 14b		97	82	55
15a	(<i>S</i>)- 15b		74	23	91
(<i>E</i>)- 18a	(<i>S</i>)- 18b		82	12	61

[a] Standard reactions (1.0 mL) were performed in buffer (50 mM KH₂PO₄/K₂HPO₄ pH 7.0) containing alkene (5 mM; added as a 2% DMF solution), NADH (6 mM) and TOYE (10 μ M) at 30 °C for 24 h at 130 rpm. [b] Conv. = % conversion. [c] by GC using DB-Wax column. [d] by GC or HPLC.

common with this substrate as seen with OPR3 and YqjM, which produced the (*S*)- and (*R*)-**14b** enantiomeric products with only 19 and 10% *ee*, respectively, due to product racemisation.^[8] Biotransformations of the citral **15a** generated citronellal (*S*)-**15b** in high optical purity (91% *ee*), but in low yield (23%). GC-MS analysis did not reveal any volatile byproducts; this suggests the low yield might result from possible side reactions that give rise to condensation products for example, nonenzymatic substrate/product decomposition in aqueous media.

The reduction of the nitroalkene (*E*)-**18a** by TOYE proceeded with a good conversion (82%) and moderate enantiopurity (61%) of the product (*S*)-**18b**, although with poor yield. By-products detected in the assays with TOYE were identified mostly as 2-phenylpropionaldehyde (that is, a Nef reaction product) with its equivalent oxime, plus some other as yet unidentified products. In addition, acetophenone was detected in both enzyme assays and the respective enzyme-free controls. Its presence suggests that substrate **18a** is relatively unstable under aqueous reaction conditions and possibly undergoes hydration followed by a retro-Henry reaction. The predominant formation of the (*S*)-enantiomer is consistent with the reactions with PETNR, NCR, OPR3 and YqjM, but opposite to those of OYE1-3 and OPR1, which produced the (*R*)-enantiomer with higher *ees*.^[8,11,14]

Biotransformations in water-miscible organic solvents

Comparative biotransformations of TOYE at 30 and 50 °C showed a reduction in both product yield and enantiopurity at high temperatures (Table S5 and see discussion "High temperature biotransformations" in the Supporting Information). Therefore we decided to exploit the improved solvent stability of thermostable TOYE. Previous studies with PETNR have shown the enantiopurity of the product (*R*)-**9b** can be dramatically improved by reaction optimisation such as a decrease in reaction time^[42] or by using biphasic solvent systems.^[42] Given the markedly increased solvent stability of TOYE over PETNR, we investigated biotransformations of TOYE with substrate **9a** at 30 °C varying the time, substrate concentration, solvent concentration and the nature of the solvent (Table 4). We used water-miscible organic solvents rather than a biphasic system to avoid the decrease in reaction rate attributed to poor mass transfer.

The effect of reaction time on the enantiopurity of the product (*R*)-**9b** shows a time-dependent loss of *ee*; this has been previously shown to be due to nonenzymatic racemisation of the product.^[42] The reactions were near completion after about 6 h; this reflects the overall slower rate of reaction seen under steady-state conditions (Table 2) compared to other OYEs^[42] as expected for a thermostable enzyme. Reaction optimisation studies of PETNR showed that for products susceptible to racemisation, a decrease in the reaction time from 24 h to 2 h was sufficient to improve the *ee* from 29% to 98%.^[42] Similar results were seen for TOYE, which showed an improvement of *ee* from 26% to 92% under these conditions. Therefore, we car-

Table 4. Product determination of the reduction of ketoisophorone **9a** to (*R*)-**9b**^[a] by TOYE in the presence of water-miscible solvent systems.

Solvent [%] ^[b]	Sub. [mM]	Time [h]	Conv. [%] ^[c]	Yield [%] ^[c]	<i>ee</i> ^[d] [%]
Time course					
DMF 2	5	0.5	13	12	> 99
DMF 2	5	1.0	37	34	95
DMF 2	5	2	71	68	92
DMF 2	5	3	89	83	88
DMF 2	5	6	96	88	76
DMF 2	5	9	97	85	64
Substrate concentration					
DMF 4	10	2	54	43	93
Solvent concentration					
DMF 5	5	2	66	64	92
DMF 10	5	2	48	42	92
DMF 15	5	2	40	32	92
DMF 20	5	2	38	23	93
DMF 30	5	2	32	12	92
Solvent comparison					
DMF 10	5	2	44	37	93
THF 10	5	2	76	69	93
MeOH 10	5	2	74	66	92
EtOH 10	5	2	70	65	95
PrOH 10	5	2	63	54	90
Acet. 10	5	2	41	36	93
ACN 10	5	2	81	66	93

[a] Standard reactions (1.0 mL) were performed in buffer (50 mM KH₂PO₄/K₂HPO₄ pH 7.0) containing water-miscible organic solvents (2–50%), ketoisophorone **9a** (5–10 mM), NADH (6 mM) and TOYE (10 μM) at 30 °C for 0.5–9 h at 130 rpm. Substrate was added to all reactions as a 2% final DMF solution. Sub.= substrate concentration; Conv.= % conversion. [b] DMF = dimethyl formamide; THF = tetrahydrofuran; MeOH = methanol; EtOH = ethanol; PrOH = propanol; Acet. = acetone; ACN = acetonitrile. [c] by GC using a DB-Wax column. [d] by GC using a Chirasil-DEX CB column.

ried out further comparative work in the presence of organic solvents by using a 2 h incubation time.

A comparison of the reduction of **9a** by TOYE in the presence of 10% water-miscible organic solvents shows that the yield of products was significantly affected by dimethylformamide (DMF), acetone and to a lesser extent by propanol (36–54% yield) compared to a 68% yield under standard reaction conditions of 2% DMF. In contrast, the presence of 10% tetrahydrofuran, methanol, ethanol and acetonitrile gave comparative conversions, yields and enantiopurities as standard reactions; this suggests the choice of cosolvent is important not only for substrate solubility but also for enzyme activity. Reactions with higher substrate and solvent concentration showed lower percent conversion for the same enzyme concentration, but increased overall yield of product; this suggests enzyme concentration optimisation is required.

We have shown that the reaction rate of TOYE decreases with increasing solvent concentration under steady-state conditions (2 min; Figure S8). To test the effect of solvent concentration under biotransformation conditions we carried out

reductions of **9a** in the presence of 2–30% DMF for 2 h at 30 °C (Table 4). As expected the percent conversion and yields decreased as the solvent concentration increased, with no effect on the product enantiopurity. While DMF is not the solvent of choice for TOYE, these results show that biotransformations can be carried out in the presence of significant quantities of water-miscible organic solvents to yield a highly enantiopure product with potentially high yields after compensatory enzyme concentration increase. Thus the higher solvent stability of TOYE compared to classical OYEs can be exploited in industrial biotransformations by using solvent concentrations normally incompatible with mesophilic enzyme structural integrity to facilitate higher substrate/product solubility.

Conclusions

We have identified and solved the structure of a novel thermostable old yellow enzyme (TOYE) and characterized its potential as an industrial biocatalyst for the asymmetric bioreduction of α,β -unsaturated ketones, aldehydes and (*E*)-1-nitro-2-phenylpropene. The enzyme forms multiple oligomeric states (tetramers to dodecamers), previously unseen among the OYE family. The relatively large active site and increased general protein and solvent stability make this enzyme a natural target for industrial-scale biotransformations. TOYE can reduce a variety of α,β -unsaturated ketones, aldehydes and the nitroalkene **18a** in a manner similar to other OYEs, although with a slightly reduced substrate range. TOYE has increased stability in water-miscible organic solvents that should be advantageous for biotransformations where water-miscible organic solvents and biphasic reaction conditions are required to deliver novel substrates to this ene-reductase catalyst.

Experimental Section

General: All reagents were of analytical grade. All the solutions for enzyme kinetics were made anaerobic and the reactions were set-up in an oxygen free environment (<5 ppm O_2). TOYE was deoxygenated by passage through a BioRad 10DG column equilibrated in anaerobic reaction buffer to avoid unproductive flavin reoxidation during oxidizing substrate reduction. The substrate extinction coefficients used were as described previously.^[44] The flavin extinction coefficient (ϵ_{456}) used for TOYE was $11\,300\text{ m}^{-1}\text{ cm}^{-1}$. The inhibitor $NADH_4$ was synthesised as described previously.^[34] Substrates and products were either obtained from Aldrich or synthesised according to the methods previously described.^[42]

Gene synthesis and mutagenesis: The protein sequence for the thermostable NADH:flavin oxidoreductase enzyme TOYE (accession number: ZP_00777979) from *T. pseudethanolicus* (ATCC 33223) was obtained from PubMed (<http://www.ncbi.nlm.nih.gov>). The gene sequence was designed and synthesised by Entelechon GmbH (Regensburg, Germany), which incorporated codon optimisation techniques of rare codon removal for optimal expression in *Escherichia coli*. The gene was cloned into pET21b (Novagen) through *Nde*I/*Xho*I restriction sites without a stop codon to incorporate a C-terminal His₆ tag. To produce a non-His₆-tag version of TOYE, a stop codon was incorporated by using the QuikChange mutagenesis strategy (Stratagene) with the primers 5'-GAACGTGCCTTCAAAAAATGAGAGCACCACCACCAC-3' and 5'-GTGGTGGTG-

GTGGTGCTCTCATTTTGAAGGCACGTTC-3' (Eurofins MWG Operon, Ebersberg, Germany). All constructs were transformed into the *E. coli* strain Arctic Express (Stratagene) for soluble protein overexpression according to the manufacturers protocol.

Protein production and purification: Native and His₆-tagged TOYE cultures were grown in Luria-Bertani medium containing the antibiotics carbenicillin ($50\text{ }\mu\text{g mL}^{-1}$) and gentamicin ($20\text{ }\mu\text{g mL}^{-1}$). Cultures were incubated at 25 °C until OD₆₀₀ reached 0.5, followed by a 12 h induction with isopropyl β -D-1-thiogalactopyranoside (IPTG; 0.4 mM) at 25 °C. Cells were harvested by centrifugation at 6000 g for 30 min at 5 °C (Beckman Coulter, Avanti J-26 XP). Cell pellets were resuspended in lysis buffer ($50\text{ mM KH}_2\text{PO}_4/\text{K}_2\text{HPO}_4$ pH 8.0) containing the EDTA-free complete protease inhibitor cocktail (Roche), DNase I (0.1 mg mL^{-1}) and lysozyme (1 mg mL^{-1}) and incubated for 30 min at 4 °C. Cells were disrupted by sonication (Sonic Vibra Cell, Newtown, CT, USA) followed by extract clarification by centrifugation for 90 min at $26\,600\text{ g}$. To improve the degree of flavination of recombinant TOYE, excess free FMN was added to the cell extracts.

Native TOYE was purified by binding to a Q-Sepharose column (50 mL ; GE Healthcare), pre-equilibrated in buffer A (50 mM Tris , pH 8.0, containing 25 mM NaCl). Proteins were separated by elution in a gradient of NaCl (25 – 200 mM) in buffer A. TOYE-His₆ was purified by binding to a Ni-NTA column (25 mL ; QIAGEN), pre-equilibrated in buffer B ($50\text{ mM KH}_2\text{PO}_4/\text{K}_2\text{HPO}_4$, pH 8.0, containing 40 mM imidazole and 0.3 M NaCl). TOYE was eluted in a step to buffer C ($50\text{ mM K H}_2\text{PO}_4/\text{K}_2\text{HPO}_4$ pH 8.0 containing 250 mM imidazole and 0.3 M NaCl). Purity was assessed by SDS-PAGE and native PAGE and the ratio of total protein versus flavinated (active) protein was determined by the BioRad (Hertfordshire, U.K.) protein assay kit according to the manufacturers protocol and using its flavin extinction coefficient, respectively. PETNR was prepared as described previously.^[11] The methods of the positive identification of all the major protein bands of purified TOYE on SDS-PAGE are described in the Supporting Information Methods.

Crystallogenes and data collection: Crystals of oxidised TOYE were grown by using the sitting-drop method in magnesium formate (50 mM) or NaOAc (0.1 M pH 4.6) containing CaCl_2 (0.2 M), isopropanol (20%) and ethylene glycol (12%) for three days at 20 °C. The crystals were soaked in mother liquor containing FMN and PEG 200 (10%), the later as a cryoprotectant, \pm saturating levels of the inhibitor $NADH_4$ and flash frozen in liquid nitrogen. Full TOYE-His₆ ($1.6\text{ }\text{\AA}$) and inhibitor-bound TOYE ($1.8\text{ }\text{\AA}$) X-ray diffraction data sets were collected from single crystals at the European Synchrotron Radiation Facility (Grenoble, France) on Station ID 14.4 (wavelength $0.97\text{ }\text{\AA}$; 100 K) by using an ADSC CCD detector.

Structure determination and refinement: Data was processed and scaled by using the programs MOSFLM^[45] and Scala.^[46] The structures were solved through molecular replacement by using the program MolRep^[46] with the coordinates for a Swiss-MODEL-generated pdb file of TOYE (<http://swissmodel.expasy.org>). This model was generated based on the known 3-D structure of the OYE Yqjm from *B. subtilis*.^[26] Model rebuilding and water addition was performed automatically by using REFMAC combined with ARP/warp.^[47] Positional and isotropic B-factor refinement was performed by using REFMAC5^[48] (hydrogens included in the refinement for the holo-TOYE structure), with alternate rounds of manual rebuilding of the model in COOT.^[48] The final models were refined to $1.60\text{ }\text{\AA}$ and $1.80\text{ }\text{\AA}$ resolution to give final $R_{\text{factor}}/R_{\text{free}}$ of $15.2/17.9$ and $15.5/19.4$ for His₆- and inhibitor-bound TOYE, respectively. The interactions involved in the subunit-subunit interfaces

were analysed by the protein interfaces, surfaces and assemblies service (PISA) at the European Bioinformatics Institute (http://www.ebi.ac.uk/msd-srv/prot_int/pistart.html).^[32] The atomic coordinates and structure factors (PDB codes 3KRU and 3KRZ for His₆- and NADH₄-PETNR structures, respectively) have been deposited in the Protein Data Bank, Research Collaboratory for Structural Bioinformatics, Rutgers University, New Brunswick, NJ (<http://www.rcsb.org/>).

Multi-angle light scattering of TOYE-His₆: TOYE was purified from its aggregates on a Supradex-200 24/30 gel filtration column (GE Healthcare) equilibrated in buffer (50 mM KH₂PO₄/K₂HPO₄, pH 7.0) on a Dionex BioLC HPLC at 0.71 mL min⁻¹. TOYE was passed through a Wyatt EOS 18-angle laser photometer with the 13th detector replaced with a Wyatt QELS detector for the simultaneous measurement of hydrodynamic radius. This was coupled to a Wyatt Optilab rEX refractive index detector and the hydrodynamic radius, molecular weight moments and concentration of the resulting peaks was analysed by using Astra 5.2.

Sedimentation velocity and bead modelling: All experiments were performed in a Beckman XL-A ultracentrifuge with an An60Ti four-hole rotor with the standard two-sector epon-filled centrepieces with quartz glass windows. All samples were purified by using gel filtration immediately prior to loading. Sedimentation of TOYE was performed in buffer (50 mM KH₂PO₄/K₂HPO₄, pH 7.0), with a rotor speed of 129024 g at 20 °C. The sedimenting boundary was monitored every 90 s at 230 nm until full sedimentation was reached. Data was interpreted with the model-based distribution of Lamm equation solutions *c*(s) using the software Sedfit^[49] and the data corrected for standard conditions of water at 20 °C by using a \bar{v} of 0.714 calculated from amino acid composition within the program Sednterp.^[50] Frictional ratios for the monomer and dimer were calculated directly from the light scattering derived mass and the sedimentation coefficient. Bead models of the quaternary structures for TOYE were generated by using the PDB file and the SOMO solution bead modelling program.^[35] The motifs were arranged in several orientations using Pymol.^[31] Multiple bead models of the TOYE domains were created in various conformations. The hydrodynamic parameters generated for the models were compared to the experimental results until a best-fit was achieved.

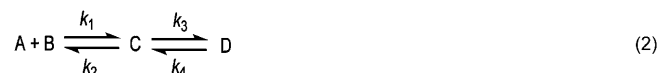
Transmission electron microscopy: TOYE-His₆ samples were absorbed onto glow discharged carbon-coated copper TEM grids and negatively stained as previously described.^[51] Data were recorded digitally by using a Joel 1220 coupled to a Gatan Orius CCD and subsequent reference free projection averaging of observed single particles was performed using EMAN (<http://blake.bcm.tmc.edu/eman/>) and strategies previously described.^[51]

Fast reaction kinetics: Reductive half-reaction kinetic experiments with both TOYE and TOYE-His₆ were performed anaerobically by using an Applied Photophysics SX.18MV-R stopped-flow spectrophotometer. The transients were analysed by using nonlinear least squares regression analysis on an Acorn Risc PC microcomputer using Spectrakinetics software (Applied Photophysics). Reactions (1.0 mL) were performed in buffer (50 mM KH₂PO₄/K₂HPO₄, pH 7.0) containing NADH or NADPH (0.05–5 mM) and TOYE (20 μM). Absorption change of flavin reduction was monitored continuously at 464 nm at 25 °C. The concentrations of substrates were always at least tenfold greater than the enzyme concentration; this ensured pseudo-first-order conditions. Each data point is the average of at least three transients. The transients were fitted to a double exponential plot (triple exponential for NADPH) from which observed

rates were determined by using the rapid equilibrium formalism of Strickland et al.^[52] (Equation 1):

$$k_{\text{ox}} = \frac{k_3[S]}{K_d + [S]} \quad (1)$$

for the kinetic scheme (Equation 2).



Steady-state kinetics: Steady-state reactions with TOYE-His₆ were performed anaerobically by using either a BioTek Synergy HT microtiter plate reader with a 0.84 cm path length or a Cary 50 Bio spectrophotometer (Varian) fitted with a temperature controlled cuvette holder. Standard reactions (0.3–1.0 mL) were performed in buffer (50 mM KH₂PO₄/K₂HPO₄, pH 7.0) containing NADPH (100 μM), oxidising substrate (0.01–1 mM; stock solutions in 100 % ethanol) and TOYE (0.1–2 μM). The reactions were followed continuously by monitoring NADPH oxidation at 340 nm (365 nm for *trans*-cinnamaldehyde) for 1 min at 25 °C. The specificity constants (apparent k_{cat}/K_M) were determined from the slope of the initial rates at oxidising substrate concentrations considerably below the estimated K_M (5–20 μM). Steady-state reactions to determine solvent stability were carried out as above (1.0 mL) in buffer (50 mM KH₂PO₄/K₂HPO₄, pH 7.0) containing NADPH (100 μM), 2-cyclohexenone (1 mM) and TOYE/PETNR (200/40 nM). The enzyme was preincubated in ethanol solutions (0–60 % ethanol in 50 mM KH₂PO₄/K₂HPO₄, pH 7.0) at 25 °C for 5 min prior to the assays. In all steady-state reactions, the final concentration of ethanol was kept constant (5 %) except in the case of activity in the presence of increasing concentrations of ethanol (5–80 %).

Biotransformations: Standard reactions (1.0 mL) were performed in buffer (50 mM KH₂PO₄/K₂HPO₄, pH 7.0) containing alkene (5 mM; added as a solution in DMF, 2 % final concentration), NAD(P)H (6 mM) and TOYE (10 μM) at 30 or 50 °C for 24 h. Additional reactions were performed as above for 2 h at 30 °C with NADH with the inclusion of the following organic solvents: dimethyl formamide, tetrahydrofuran, ethanol, methanol, propanol, acetone and acetonitrile (2–30 % v/v). The products were extracted and analysed for percent yield, percent conversion and enantiomeric excess according to methods previously described.^[42]

Circular dichroism: Circular dichroism (CD) measurements of TOYE-His₆ were performed by using a Chirascan CD spectrometer (Applied Photophysics, UK) with a thermoelectrically controlled cell holder and a 2 mm path length cuvette. Secondary structure unfolding of TOYE (5–10 μM in 50 mM KH₂PO₄/K₂HPO₄, pH 7.0) was monitored by absorbance change at 222 nm over time (1 h) between 70–80 °C and analysed by the Pro-Data Chirascan software. Data is corrected for background solvent effects and expressed as percent signal strength.

Differential scanning calorimetry: TOYE (0.5 mg mL⁻¹) was denatured under controlled conditions to monitor the melting temperature (T_m) of the protein and its domains and the enthalpy of the unfolding event (ΔH_V). This was performed using a VP-DSC instrument (MicroCal) with a scan rate of 60 °C h⁻¹ from 20 °C to 100 °C. Protein samples were purified by using gel filtration chromatography and referenced using the column buffer. Data was analyzed using Microcal ORIGIN software (Microcal Inc., Amherst, MA).

Fluorescence spectroscopy: Temperature-induced unfolding of the protein was monitored by using either tryptophan or flavin intrinsic fluorescence on a Jasco FP750 spectrofluorimeter fitted with an external heating/cooling water bath. Tryptophan fluorescence was studied with an excitation of 295 nm and scanning between 310 and 400 nm. Flavin fluorescence was studied by using an excitation of 430 nm and scanning emissions between 460 and 600 nm. Temperature-induced unfolding was achieved by a 20 min incubation of 5 μ M TOYE within the instrument at 10 degree intervals between 20 °C and 80 °C with each protein sample scanned once only.

Acknowledgements

We thank Richard Collins for the electron microscopy data and Emma Keevill for the mass spectrometry protein identification analysis. This work was funded by UK Biotechnology and Biological Sciences Research Council (BBSRC). N.S.S. is a BBSRC Professorial Research Fellow.

Keywords: asymmetric bioreduction • biocatalysis • thermostable enzymes • unsaturated alkenes • UV/Vis spectroscopy • X-ray crystallography

- [1] S. Panke, M. Held, M. Wubbolts, *Curr. Opin. Biotechnol.* **2004**, *15*, 272–279.
- [2] J. A. Littlechild, J. Guy, S. Connelly, L. Mallett, S. Waddell, C. A. Rye, K. Line, M. Isupov, *Biochem. Soc. Trans.* **2007**, *35*, 1558–1563.
- [3] S. Luetz, L. Giver, J. Lalonde, *Biotechnol. Bioeng.* **2008**, *101*, 647–653.
- [4] G. R. Castro, T. Knubovets, *Crit. Rev. Biotechnol.* **2003**, *23*, 195–231.
- [5] C. Breithaupt, *EMBO Rep.* **2001**, *2*, 968–971.
- [6] M. Champdoré, M. Staiano, M. Rossi, S. D'Auria, *J. R. Soc. Interf.* **2007**, *4*, 183–191.
- [7] L. D. Unsworth, J. van der Oost, S. Koutsopoulos, *FEBS J.* **2007**, *274*, 4044–4056.
- [8] M. Hall, C. Stueckler, H. Ehammer, E. Pointner, G. Oberdorfer, K. Gruber, B. Hauer, R. Stuermer, W. Kroutil, P. Macheroux, K. Faber, *Adv. Synth. Catal.* **2008**, *350*, 411–418.
- [9] M. Hall, C. Stueckler, B. Hauer, R. Stuermer, W. Kroutil, P. Macheroux, K. Facer, in *Biotrans-8th International Symposium on Biocatalysis and Bio-transformations*, Oviedo, Spain, **2007**.
- [10] M. Hall, C. Stueckler, W. Kroutil, P. Macheroux, K. Faber, *Angew. Chem.* **2007**, *119*, 4008–4011; *Angew. Chem. Int. Ed.* **2007**, *46*, 3934–3937.
- [11] H. S. Toogood, A. Fryszkowska, V. Hare, K. Fisher, A. Roujeinikova, D. Leys, J. M. Gardiner, G. M. Stephens, N. S. Scrutton, *Adv. Synth. Catal.* **2008**, *350*, 2789–2803.
- [12] D. J. Bougioukou, J. D. Stewart, *J. Am. Chem. Soc.* **2008**, *130*, 7655–7658.
- [13] J. F. Chaparro-Riggers, T. A. Rogers, E. Vazquez-Figueroa, K. M. Polizzi, A. S. Bommaris, *Adv. Synth. Catal.* **2007**, *349*, 1521–1531.
- [14] M. Hall, C. Stueckler, B. Hauer, R. Stuermer, T. Friedrich, M. Breuer, W. Kroutil, K. Faber, *Eur. J. Org. Chem.* **2008**, 1511–1516.
- [15] S. K. Padhi, D. J. Bougioukou, J. D. Stewart, *J. Am. Chem. Soc.* **2009**, *131*, 3271–3280.
- [16] C. Stueckler, M. Hall, H. Ehammer, E. Pointner, W. Kroutil, P. Macheroux, K. Faber, *Org. Lett.* **2007**, *9*, 5409–5411.
- [17] M. A. Swiderska, J. D. Stewart, *J. Mol. Catal. B* **2006**, *42*, 52–54.
- [18] M. A. Swiderska, J. D. Stewart, *Org. Lett.* **2006**, *8*, 6131–6133.
- [19] O. Warburg, W. Christian, *Naturwissenschaften* **1932**, *20*, 688.
- [20] P. R. Binks, C. E. French, S. Nicklin, N. C. Bruce, *Appl. Environ. Microbiol.* **1996**, *62*, 1214–1219.
- [21] C. E. French, N. C. Bruce, *Biochem. J.* **1995**, *312*, 671–678.
- [22] B. A. Vick, D. C. Zimmerman, *Plant Physiol.* **1986**, *80*, 202–205.
- [23] T. B. Fitzpatrick, N. Amrhein, P. Macheroux, *J. Biol. Chem.* **2003**, *278*, 19891–19897.
- [24] P. A. Karplus, K. M. Fox, V. Massey, *FASEB J.* **1995**, *9*, 1518–1526.
- [25] T. Barna, H. L. Messiha, C. Petosa, N. C. Bruce, N. S. Scrutton, P. C. E. Moody, *J. Biol. Chem.* **2002**, *277*, 30976–30983.
- [26] K. Kitzing, T. B. Fitzpatrick, C. Wilken, J. Sawa, G. P. Bourenkov, P. Macheroux, T. Clausen, *J. Biol. Chem.* **2005**, *280*, 27904–27913.
- [27] R. U. Onyenwoke, V. V. Kevbrin, A. M. Lysenko, J. Wiegel, *Int. J. Syst. Evol. Microbiol.* **2007**, *57*, 2191–2193.
- [28] T. N. Nazina, T. P. Tourova, A. B. Poltarau, E. V. Novikova, A. A. Grigoryan, A. E. Ivanova, A. M. Lysenko, V. V. Petrunyaka, G. A. Osipov, S. S. Belyaev, M. V. Ivanov, *Int. J. Syst. Evol. Microbiol.* **2001**, *51*, 433–446.
- [29] F. A. Rainey, E. Stackebrandt, *Int. J. Syst. Bacteriol.* **1993**, *43*, 857–859.
- [30] P. R. Binks, C. E. French, S. Nicklin, N. C. Bruce, *Appl. Environ. Microbiol.* **1996**, *62*, 1214–1219.
- [31] W. L. DeLano, DeLano Scientific, Palo Alto, CA, USA, **2002**.
- [32] E. Krissinel, K. Henrick, *J. Mol. Biol.* **2007**, *372*, 774–797.
- [33] T. M. Barna, H. Khan, N. C. Bruce, I. Barsukov, N. S. Scrutton, P. C. E. Moody, *J. Mol. Biol.* **2001**, *310*, 433–447.
- [34] C. R. Pudney, S. Hay, J. Y. Pang, C. Costello, D. Leys, M. J. Sutcliffe, N. S. Scrutton, *J. Am. Chem. Soc.* **2007**, *129*, 13949–13956.
- [35] N. Rai, M. Nollmann, B. Spotorno, G. Tassara, O. Byron, M. Rocco, *Structure* **2005**, *13*, 723–734.
- [36] R. M. Daniel in *Protein Structure, Folding and Design*. (Ed.: D. L. Oxender), Alan R. Liss, New York, **1986**, pp. 291–296.
- [37] A. Guagliardi, G. Manco, M. Rossi, S. Bartolucci, *Eur. J. Biochem.* **1989**, *183*, 25–30.
- [38] H. Huber, K. O. Stetter, *J. Biotechnol.* **1998**, *64*, 39–52.
- [39] R. K. Owusu, D. A. Cowan, *Enzym. Microb. Technol.* **1989**, *11*, 568–574.
- [40] R. Stuermer, B. Hauer, M. Hall, K. Faber, *Curr. Opin. Chem. Biol.* **2007**, *11*, 203–213.
- [41] T. B. Fitzpatrick, S. Auweter, K. Kitzing, T. Clausen, N. Amrhein, P. Macheroux, *Protein Expression Purif.* **2004**, *36*, 280–291.
- [42] A. Fryszkowska, H. S. Toogood, M. Sakuma, J. M. Gardiner, G. M. Stephens, N. S. Scrutton, *Adv. Synth. Catal.* **2009**; DOI: 10.1002/adsc.200900574.
- [43] R. C. Stewart, V. Massey, *J. Biol. Chem.* **1985**, *260*, 13639–13647.
- [44] A. Fryszkowska, K. Fisher, J. M. Gardiner, G. M. Stephens, *J. Org. Chem.* **2008**, *73*, 4295–4298.
- [45] A. G. W. Leslie in *Joint CCP4 & ESRF-EACBM Newsletter on Protein Crystallography*, Serc Laboratory, Daresbury, Warrington, U.K. **1992**.
- [46] Collaborative Computational Project, Number 4, *Acta Crystallogr. Sect. D: Biol. Crystallogr.* **1994**, *50*, 760–763.
- [47] A. Perrakis, R. Morris, V. S. Lamzin, *Nat. Struct. Biol.* **1999**, *6*, 458–463.
- [48] P. Emsley, K. Cowtan, *Acta Crystallogr. Sect. D* **2004**, *60*, 2126–2132.
- [49] P. Schuck, *Biophys. J.* **2000**, *78*, 1606–1619.
- [50] D. Hayes, J. J. Philo, *Sednterp*, University of New Hampshire, New Hampshire, **1992**.
- [51] R. F. Collins, M. Saleem, J. P. Derrick, *J. Bacteriol.* **2007**, *189*, 6389–6396.
- [52] S. Strickland, G. Palmer, V. Massey, *J. Biol. Chem.* **1975**, *250*, 4048–4052.

Received: September 11, 2009

Published online on November 26, 2009